



Exponential growth of electrochemical double layer capacitance in glassy carbon during thermal oxidation

A. Braun^{a,b,*}, M. Bärtsch^a, O. Merlo^{a,c}, B. Schnyder^a, B. Schaffner^b, R. Kötze^a, O. Haas^a, A. Wokaun^{a,b}

^aPaul Scherrer Institute, General Energy Research Department, CH-5232 Villigen PSI, Switzerland

^bDepartment of Chemical Engineering and Industrial Chemistry, Swiss Federal Institute of Technology, ETH Zentrum, CH-8092 Zürich, Switzerland

^cUniversité Fribourg, Département de Physique Théoriques, Chemin du Musée 3, CH-1700 Fribourg, Switzerland

Received 14 September 2001; accepted 29 October 2002

Abstract

The evolution of the electrochemical double layer capacitance of glassy carbon during thermochemical gas phase oxidation was studied with electrochemical impedance spectroscopy. Particular attention was paid to the initial oxidation stage, during which the capacitance grows exponentially. This stage could be experimentally assessed by lowering the reaction temperature and oxidant partial pressure. After a specific oxidation time the capacitance growth experiences a cross-over to a logistic growth.

© 2002 Elsevier Science Ltd. All rights reserved.

Keywords: A. Glass-like carbon; B. Activation; D. Microporosity; Electrochemical properties

1. Introduction

Glassy carbon (GC) is a carbon material with voids of about 1 to 2 nm diameter, which are closed and separated against each other [1,2]. The voids (pores) can be opened by thermochemical gas phase oxidation (*activation*) [3–9]. The opened pores then become accessible to gases and liquids and provide a huge specific internal surface area. Such activated GC can be utilized as an electrode material for electrochemical double layer capacitors [3,6,7,10–12].

The activation creates a film with open pores on the surface region of the GC, which envelopes the non-activated, impermeable interior material [4–7]. We found that the film growth is a chemical process controlled by the diffusion of reactants and products [5–7,9,13]. The film growth is superimposed by a second process, which burns off the film due to combustion. This process is controlled

by the chemical reaction of the carbon with the oxidant [5–7,9,13].

We have recently reported results on the film growth of GC during thermal activation [4,6,8,9,13]. In these publications, a model for the growth of the active film and the decrease of the sample thickness was presented, and experimental data were compared with the model predictions. The model was based on the assumption that the film growth was confined to a sharp interface between film and bulk, and the interface propagates into the sample interior. The activation of glassy carbon therefore represents a case of a predator–prey system [14].

The double layer capacitance of activated GC per activated sample (film) *volume* was found to be essentially constant during activation [4]. Only a slight increase of the volumetric capacitance of about 10% per hour was found and could be ascribed to pore enlargement during activation [4]. Therefore, for longer activation times, the evolution of the overall capacitance per geometric sample *area* essentially reflects the growth of the active film thickness.

To determine the internal surface area and porosity, gas adsorption measurements [4,6,7] and X-ray scattering [4,6–8] and gravimetric experiments [7] had been carried out and were already reported. Results for the surface area

*Corresponding author. Present address: Consortium for Fossil Fuel Science, University of Kentucky, Suite 107, S. Whalen Building, 533 South Limestone Street, Lexington, KY 40502, USA. Tel.: +1-859-257-6087; fax: +1-859-257-7215.

E-mail address: Artur.Braun@alumni.ethz.ch (A. Braun).

obtained by those techniques for the same samples are in fair agreement.

In particular, we found a linear correlation between internal surface area and double layer capacitance [4], which gives an indication that the surface condition in the activated GC is basically independent from its oxidation condition.

These findings differ significantly from previously published data [15] that treated a different system, that was, *electrochemical* activation of a different kind of GC. In particular, unlike for electrochemical activation, thermochemical activation requires no subsequent reduction to obtain a reasonably high capacitance.

Phenomenologically, the evolution of film thickness and capacitance per apparent sample area can be described by a square-root-shaped function, which, however, converges to a constant value for large activation times. This growth behavior is a manifestation of the diffusion limitation during activation and particularly well observed for higher oxidant pressures and higher temperatures.

However, growth of the active film is connected with the evolution of open porosity and accessible internal surface area, which is a continuous process taking place in the entire film and not only at the interface between film and unreacted core.

We now report results found on samples activated only for a short time at low temperature or at low oxygen pressure, which exhibit an exponential growth of the capacitance.

Such a growth behavior represents the process of a normal reproduction [14], that is, the growth rate is constant and the change in internal surface area is proportional to the surface area already present. The present work addresses the evolution of the volumetric accessible internal surface area during the *initial* stage of activation.

Note that the diffusion limitation of the activation yields a decreasing reaction rate; this is the logistic growth.

2. Experimental

2.1. Sample preparation

GC sheets of 1000 microns thickness were investigated. The samples were cut into rectangular pieces measuring about 1 cm×2 cm. The thermochemical oxidation was carried out in a muffle furnace as described in Ref. [3]. As an oxidant, mixtures of oxygen and nitrogen in four different mixing ratios were used: 0.05 bar O₂ and 0.95 bar N₂, and corresponding mixtures with 0.2 bar and 0.5 bar oxygen partial pressure, and also oxygen with no nitrogen added.

After a specified time, the first sample of a set was removed from the furnace, while the remaining samples of the set were kept in the furnace. Later, the second sample was removed, and so on. So a set of samples, all activated

at one particular temperature as described in Ref. [3] but for different activation times, could be provided. Once removed from the furnace, the hot samples cooled down quickly at ambient atmosphere.

2.2. Electrochemical measurements

Each of the activated samples was contacted with a gold-plated brass sample holder and covered with varnish, with the exception of a free area used for the measurements, the latter being the only GC area subsequently exposed to the electrolyte. Experiments were carried out in 3 M H₂SO₄ using a Potentiostat/Galvanostat (EG&G 273 A) and an Impedance/Gain-Phase Analyzer (Solartron SI 1260).

Prior to capacitance measurements, a cyclic voltammogram of the activated sample was recorded with a scan rate of $\nu = 10$ mV/s over a potential range from 0.00 to 1.00 V vs. saturated calomel electrode (SCE) in order to check the electrochemical system for cleanliness and to obtain a stable electrochemical system. Electrochemical impedance spectra (EIS) were recorded at a potential of 0.9 V vs. SCE over a frequency range from 0.1 Hz to 100 kHz.

From the imaginary part of the impedance, $Im(Z)$, the specific double layer capacitance $C_A(f)$ (farad/cm²) of the sample with the exposed area A was determined for the frequency $f = 0.1$ Hz using the following relation:

$$C_A(f) = \frac{-1}{2\pi f Im(Z)A}. \quad (1)$$

3. Results

3.1. Variation of temperature

Fig. 1 displays the capacitance per sample area for samples activated with 0.2 bar oxygen partial pressure (p_{O_2}) at four different temperatures, for times up to 180 min.

The capacitance of the samples activated at the lowest temperature ($T_0 = 350$ °C) can be described by a linear function in the semi-log plot, and thus, in linear axis, by an exponential. Each of the plots in Fig. 1 has an inset, which shows the data with linear axes.

A conceptual verification for the introduction of an exponential will be given in the Discussion.

For samples activated for 3 h at 350 °C, a rather low capacitance has been observed, which is still far below the saturation value. This saturation value can be obtained after longer activation. However, samples activated at short times such as 30, 60, and 90 min, were relatively difficult to measure and show a deviation from the exponential trend.

GC activated at T_1 (400 °C) shows a pronounced exponential increase of the capacitance during the first 90

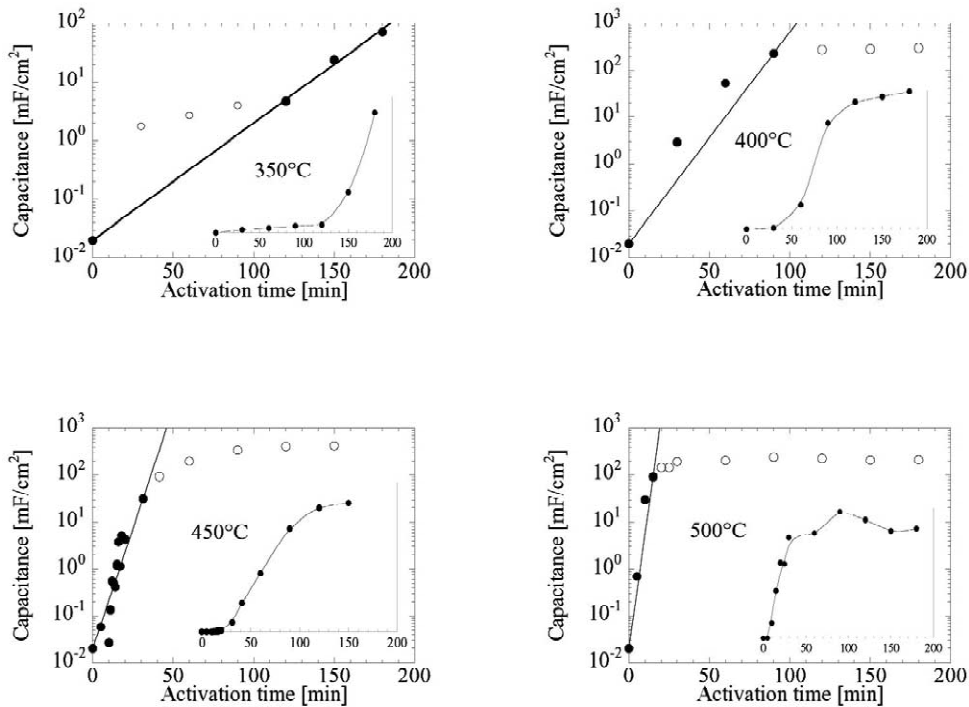


Fig. 1. Capacitance of samples (inset shows linear axes), activated at four different temperatures. The drawn line is the exponential least square fit (Eq. (2)) to these data points.

min of activation. At about this time, the convex, exponential growth profile changes to a concave, square-root-like profile (see inset), such as when the capacitance would be approaching a saturation value.

The exact same trend is observed for the samples activated at T_2 (450 °C); however, compared with T_1 , the curve profile is shifted by about 30 min towards shorter times when we compare the insets. This indicates that the change of the growth profiles takes place already after 60 min of activation. Even more remarkable, the slope of the exponential increases by a factor of roughly two.

At temperature T_3 (500 °C), the change of growth mode already takes place during the first 15 min of activation.

For all curves, an exponential could be fitted to selected data points according to the following relation:

$$C(t) = C_0 \cdot \exp(kp_{O_2}t), \quad (2)$$

with an initial capacitance of C_0 , which should be around 20 $\mu\text{F}/\text{cm}^2$ [4,6], p_{O_2} being the partial pressure of oxygen, and k a reaction rate constant depending on the temperature by Arrhenius' law:

$$k(T) = k_{T \rightarrow \infty} \exp\left(-\frac{E_A}{RT}\right). \quad (3)$$

To identify the range of exponential growth and select appropriate data points, the data were plotted on a semi-

logarithmic axis, as shown in Fig. 1. Those data points, which indicate the exponential growth, are marked with filled symbols and are positioned on an approximately straight line in a semi-logarithmic plot. An exponential fit was applied to the selected original data as marked by filled symbols.

The four reaction rates for the activation process obtained for temperatures T_0 to T_3 are displayed in Fig. 2 in Arrhenius representation. The linear least square fit of the

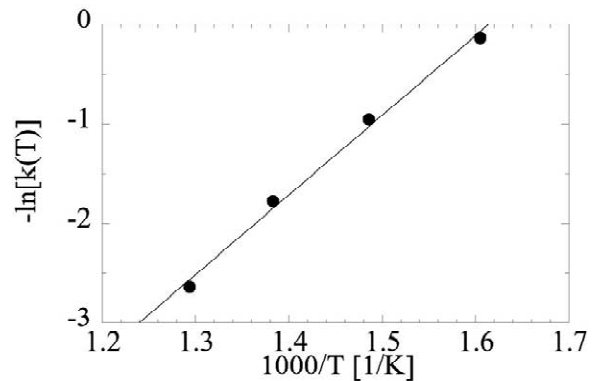


Fig. 2. Reaction rate constants for reaction temperatures T_0 to T_3 as obtained from the fit of an exponential to the capacitance data in Fig. 1. The straight line is a linear least square fit to the data points.

four data points yields a ratio of 8.028×10^3 K for E_A/R , with the gas constant $R = 8.314$ J mol⁻¹ K⁻¹. This corresponds to an activation energy E_A of 66.95 kJ/mol which exceeds the literature data of 54.4 kJ/mol [1] for carbon combustion by about 23%.

With $p_{O_2} = 0.2$ bar, the reaction rate constant at 450 °C was determined as 5.63 bar⁻¹ min⁻¹.

The determination of the capacitance, and thus its growth behavior, is based on the presence of pores wide enough for the electrolyte ions. Pores, which are opened by the activation process, but too small for the electrolyte to penetrate, do not contribute to the capacitance. Consequently, the activation energy is overestimated, which partially explains the discrepancy to the literature value.

3.2. Variation of oxygen pressure

Fig. 3 displays the capacitance of GC activated at 450 °C, but at four different oxygen partial pressures.

The data points in the upper left part of Fig. 3 were obtained from samples activated at $p_{O_2} = 0.05$ bar. The first six data points (up to 150 min) can be represented by a linear fit. These data points are marked as filled circles and exhibit an exponential growth, since they are on a straight line in the semi-logarithmic plot.

For the data obtained at $p_{O_2} = 0.2$ bar, the range of exponential growth was 30 min, and an exponential was fitted to the data in this range as well. From the samples activated at $p_{O_2} = 0.5$ bar (1 bar), 30 min (10 min) was found as the appropriate range to apply the exponential fit.

We continue with the same approach as was already carried out for the reaction rate in the temperature studies (Eq. (2)):

$$C(t) = C_0 \cdot \exp(k^* p_{O_2} t). \quad (4)$$

The reciprocal of the product ($k^* p_{O_2}$) can be interpreted as a time constant τ ,

$$\frac{1}{\tau} = k^* p_{O_2} \quad (5)$$

such that

$$C(t) = C_0 \exp\left(\frac{t}{\tau}\right). \quad (6)$$

Values for the slope obtained from the data in Fig. 3 are listed in Table 1 (in the form of τ). The value of $1/\tau$ increases as the oxygen pressure increases. This means that the rate of activation increases when the oxygen pressure is increased. This experimental finding is expected and in

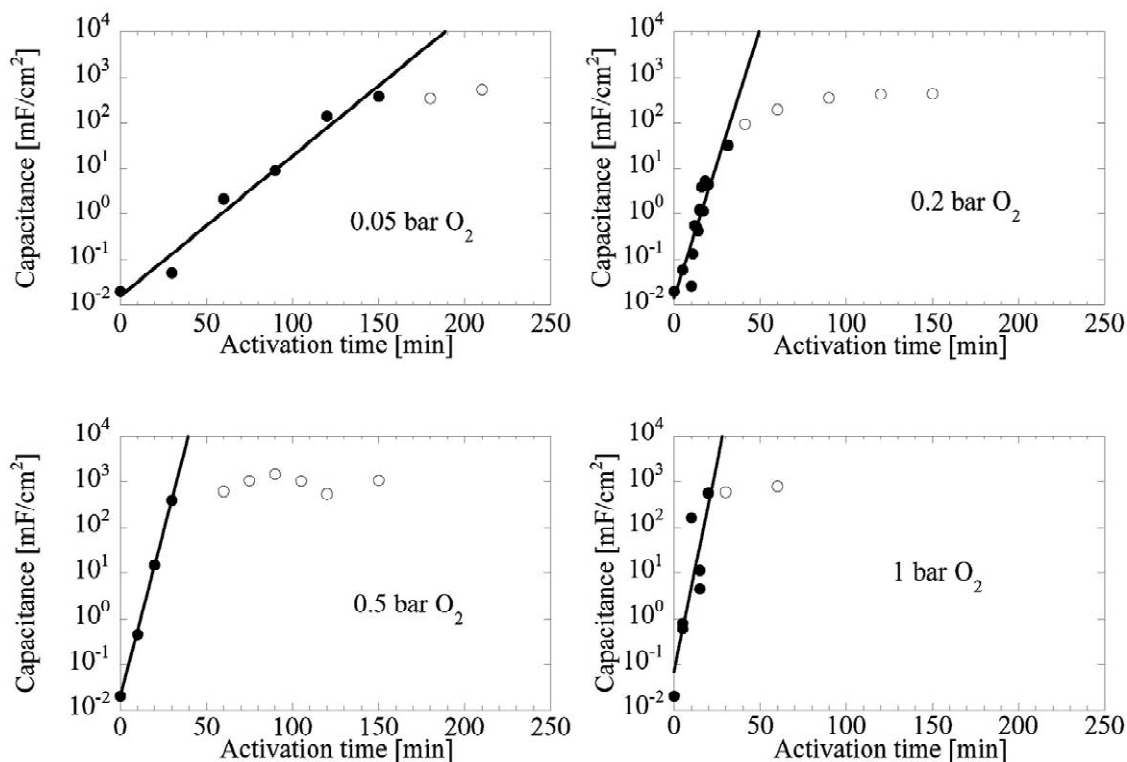


Fig. 3. Capacitance per apparent sample surface area (mF/cm²) for four different p_{O_2} , after activation at 450 °C. The drawn line is the exponential least square fit (Eq. (4)) of these data points.

Table 1

Capacitance, time of exponential growth, initial capacitance C_0 and time constant τ of GC for various p_{O_2} . C_0 and τ were obtained by fitting Eq. (4) to the data points in Fig. 3

p_{O_2} (bar)	Time (min)	Capacitance C_0 ($\mu\text{F}/\text{cm}^2$)	τ (min)
0	–	20.0	$\rightarrow\infty$
0.05	150	15.5	14.1
0.2	30	20.0	3.7
0.5	30	18.7	3.0
1	20	12.9	2.4

line with the predictions of the mathematical model published in Refs. [9,13].

We include in Table 1 also the trivial data point for the activation with no oxidant at all. The values for k^* are summarized in Table 1, together with k from the temperature studies. We note, however, that the values for k^* obtained from samples activated at $p_{O_2}=0.5$ and 1 bar may be somewhat doubtful (0.66 and 0.42, respectively), because the range of exponential growth under such strong activation conditions could not be determined unambiguously.

4. Discussion

For samples activated only weakly (short time of activation either at low temperatures or with low p_{O_2}), it is observed that the capacitance per sample area increases not square-root-like but exponentially.

The exponential part of the growth was not observed in our previously reported film thickness studies on the same material [9,13]. In these studies only a square-root-like increase of film thickness during activation was found, and we were able to quantitatively model the film thickness evolution of the samples during activation within the limitations of the extended *unreacted core model*. Our extended model took even the shrinking of the entire sample during activation into account.

We exclude the trivial case where, when a thin GC sample is considered, the films on either sample side may become so thick that the unreacted core finally vanishes and the two films meet in the center of the sample. This stage is actually observed after 3 h of activation at 450 °C.

The evolution of the film thickness within this model can be described by the so-called *Generalized LambertW Function* \mathcal{G} [9,13,16], which mainly accounts for the diffusion-controlled nature of the activation process. The curvature of \mathcal{G} is thus similar to a square-root function, with the distinctive feature however that it tends to a constant saturation film thickness for infinite activation times, unlike the square-root function, which diverges for its infinite arguments. The shrinking of the entire sample

during activation is the origin of this feature. We refer the reader to Figs. 1–3 in Ref. [4], Fig. 3 in Ref. [5], Figs. 1–4 in Ref. [9], and Fig. 1 in Ref. [13] for drawings and schematics about the film growth.

The first analytical derivation of \mathcal{G} is given by Briggs [16]. We note that the series expansion of \mathcal{G} simplifies to an exact square-root growth law, when the burn off rate is taken as zero [9,13].

Experimentally, the saturation thickness is proportional to the ratio of the diffusion coefficient and the reaction rate, as also observed for the experimental film thickness data [9].

According to the observations made on the film thickness growth [4,9,13], which exhibits a square-root-like behavior with an oxidation time due to the properties of \mathcal{G} , the evolution of the capacitance should exhibit the same behavior. Here we implicitly assume a linear correlation between internal surface area and double layer capacity. In fact, a linear correlation between internal surface area and double layer capacity was found in one of our recent studies [4] on activated glassy carbon.

However, the square-root-like growth, as found in this study, seems not to be recovered when the activation is retarded due to low temperature or low p_{O_2} . Experimentally, we find a growth of capacitance, which can be expressed by an exponential and thus appears like the growth of a normal reproduction.

Only for longer activation times or higher oxidant pressure, the curves for the capacitance follow the \mathcal{G} behavior.

Obviously there is a crossover from the growth of normal reproduction to a logistic growth [14].

The exponential part of the curve is particularly well resolved for samples either activated with low p_{O_2} or at low activation temperature. While the temperature studies give a fairly consistent trend for k , the reaction rate constants k^* for 0.5 bar and 1 bar in the pressure studies seem to be underestimated (Table 2). One likely origin for that could be that diffusion limitation plays already a significant role under those conditions.

We believe that the stage of *normal reproduction* of the activation is present during the entire activation process, and that its range extends from the interface of the unreacted core/film into the film for a characteristic length which we call *range* of activation. Both the boundary and the range propagate during activation into the sample

Table 2

Reaction rate constants k (k^*) ($\text{bar}^{-1} \text{min}^{-1}$) for the temperature (pressure) studies

$T; p_{O_2}$	0.05 bar	0.2 bar	0.5 bar	1.0 bar
350 °C	–	0.23	–	–
400 °C	–	0.52	–	–
450 °C	1.42	1.25	0.66	0.42
500 °C	–	2.81	–	–

interior within the framework of a logistic growth problem (diffusion controlled, \mathcal{G} function). The stage of normal reproduction is probably the opening and widening of the pores in the glassy carbon, which originally were closed.

It is throughout likely that the structure and the porosity of the GC in this range have a gradient, just as its mass density could also have a gradient. We have studied one partially activated GC plate of 60 microns thickness, with a film thickness of 11 microns after 1 h of activation with air at 450 °C. An optical Raman line profile scan was applied to the fracture cross section of that sample. The scattered intensity over the film followed a linear profile, while the profile over the unreacted core was constant. This linear profile can arise from a linear porosity gradient, which is the common origin of the square-root-like curvature of the film thickness evolution. However, within the limits of spatial resolution of the Raman microscope (1 μm) which we employed, no deviation from the linear profile was found in the vicinity of the interface between unreacted core and film.

The stage of normal reproduction could also not be identified with scanning electron microscopy although this technique was successfully applied to determine the overall film thickness [4,6,9].

Further experimental evidence for a difference between the film and the interface between film and unreacted core is provided by electrochemical impedance data, which show that the so-called electrochemical diffusion resistance of the electrolyte, which is confined by the pores, is significantly high for samples activated only short times at low temperatures [4,6]. Upon further activation, the diffusion resistance decreases by several orders of magnitude to a minimum.

One explanation for this effect could be that, at the initial stage of activation, the pore entries are too small for the electrolyte to penetrate, acting as a bottleneck, which results in the high diffusion resistance of the electrolyte.

At this early stage of activation, pore walls would be thinned by oxidation, and thus pores will grow. Therefore, the internal surface area will increase accordingly. Finally, at later stages of activation, the pore walls will vanish due to oxidation, and the internal surface area will decrease again.

Hence, a proportionality between mass loss and increasing internal surface area is justified for the early stage of oxidation.

The latter effect (decreasing surface area) was reported in our previous studies [4,6], the former effect (increasing surface area) is the subject of the present work.

We give a brief derivation of how the capacitance follows an exponential growth.

Assuming that the change of the internal surface area at initial stage of reaction is proportional to the mass loss, and the mass loss is proportional to the surface already available, the following relations hold:

$$\frac{dA}{dt} \sim - \frac{dm}{dt} = k^{**} p_{\text{O}_2} A, \quad (7)$$

where A is the surface area and m is the mass of GC, k^{**} is the reaction rate constant, p_{O_2} is the partial pressure of oxygen. It follows

$$\frac{dC}{dt} = k p_{\text{O}_2} C \quad (8)$$

where C is the capacitance and k is also a reaction rate constant, which differs from k by a constant factor only. Separation of variables C and t and integration yields the solution

$$C(t) = C_0 \cdot \exp(k p_{\text{O}_2} t). \quad (9)$$

Therefore, during the initial stage the growth follows an exponential.

5. Conclusions

Glassy carbon samples were thermochemically activated, and their electrochemical double layer capacitance was determined with impedance spectroscopy. By lowering the activation temperature and partial pressure of oxidant gas we have retarded the activation so far that we were able to discriminate between the evolution of the volumetric internal surface area and the diffusion-controlled propagation of the active film into the sample interior.

The exponential growth mode of the former process can be interpreted as a normal reproduction of the internal surface area in GC, as a result of pore opening and widening. It is likely that the major structural changes of the GC during activation occur within this exponential growth regime. However, additional direct experimental techniques are desirable to elucidate the structural changes during activation, in particular the opening and widening of the pores in particular depth ranges of the samples.

As long as the logistic growth regime is not reached yet, the diffusion resistance of electrodes from such materials is significantly high, probably because the pores are still too narrow for the electrolyte to penetrate easily. Once a sufficient number of pores is opened and accessible for the electrolyte, the diffusion resistance decreases and then the material can be used as an electrode for electrochemical double layer capacitors.

Acknowledgements

This research was financially supported by the Board of the Swiss Federal Institute of Technology within the Swiss Priority Program on Materials Research. We are grateful to J.-C. Panitz (PSI) for the Raman microscopy experiment. Fruitful collaboration with ABB Corporate Research, Baden (Switzerland), and Leclanché S.A., Yverdon Les Bains (Switzerland), is gratefully acknowledged.

References

- [1] Jenkins GM, Kawamura K. In: 1st ed, Polymeric carbons—carbon fibre, glass and char, Cambridge, UK: Cambridge University Press, 1976.
- [2] Lewis JC, Redfern B, Cowland FC. Solid-State Electron 1963;6(3):251–5.
- [3] Miklos J, Mund K, Naschwitz W, Siemens AG, Offenlegungsschrift DE 30 11 701 A1, Deutsches Patentamt, 1980.
- [4] Braun A, Bärtsch M, Schnyder B, Kötzt R, Haas O, Goerigk G et al. X-ray scattering and adsorption studies of thermally oxidized glassy carbon. J Non-Cryst Solids 1999;260(1–2):1–14.
- [5] Braun A, Bärtsch M, Schnyder B, Kötzt R, Haas O, Wokaun A. Evolution of BET internal surface area in glassy carbon powder during thermal oxidation. Carbon 2002;40(3):375–82.
- [6] Braun A, Bärtsch M, Geiger F, Schnyder B, Kötzt R, Haas O et al. A study on oxidized glassy carbon sheets for bipolar supercapacitor electrodes. Proc Mater Res Soc Spring Meet 1999;575:369–80.
- [7] Braun A. Dissertation no. 13292. Zürich: ETH, 1999.
- [8] Gille W, Braun A. SAXS chord length distribution analysis and porosity estimation of activated and non-activated glassy carbon. J Non-Cryst Solids, in press.
- [9] Braun A, Bärtsch M, Schnyder B, Kötzt R. A model for the film growth in samples with two moving reaction frontiers—an application and extension of the unreacted-core model. Chem Eng Sci 2000;55(22):5273–82.
- [10] Kötzt R, Carlen M. Principles and applications of electrochemical capacitors. Electrochim Acta 2000;45(15–16):2483–98.
- [11] Bärtsch M, Braun A, Kötzt R, Haas O. High-power electrochemical double-layer capacitor. In: Proceedings of the 38th power sources conference, Cherry Hill, NJ, 1988.
- [12] Bärtsch M, Braun A, Schnyder B, Kötzt R, Haas O. Bipolar glassy carbon electrochemical double-layer capacitor: 100,000 cycles demonstrated. J New Mater Electrochem Syst 1999;2(4):273–7.
- [13] Braun A, Wokaun A, Hermanns H-G. Analytical solution to a growth problem with two moving boundaries. Appl Math Model 2003;27(1):47–52.
- [14] Arnol'd VI. Ordinary differential equations, §1, examples 6 and 8. Springer Verlag, 1992.
- [15] Sullivan MG, Schnyder B, Bärtsch M, Allia D, Barbero C, Imhof R et al. Electrochemically modified glassy carbon for capacitor electrodes. J Electrochem Soc 2000;147(7):2636–43.
- [16] Briggs KM. Some exactly solvable growth problems. In preparation.